Journal of Alloys and Compounds 685 (2016) 957–961

Contents lists available at ScienceDirect

Journal of Alloys and Compounds

journal homepage: http://www.elsevier.com/locate/jalcom

Crystal structure and physical properties of Yb_2PdGe_6

D. Kaczorowski [a], A.V. Gribanov [b, *], P. Rogl [c], S.F. Dunaev [b]

[a] Institute of Low Temperature and Structure Research, Polish Academy of Sciences, P.O. Box 1410, 50-950, Wrocław, Poland
[b] Chemistry Department of the Moscow State University, Leninskie Gory, GSP-1, 119991, Moscow, Russia
[c] Institute of Material Chemistry and Research, University of Vienna, Währingerstrasse42, A-1090, Wien, Austria

ARTICLE INFO

Article history:
Received 20 May 2016
Received in revised form
21 June 2016
Accepted 22 June 2016
Available online 25 June 2016

Keywords:
Ytterbium intermetallics
Crystal structure
Magnetic properties
Electrical transport
Valence fluctuations

ABSTRACT

The crystal structure of Yb_2PdGe_6 was studied by powder X-ray diffraction technique. The compound in both as-cast and annealed forms crystallizes with the orthorhombic structure of the Ce_2GaGe_6-type (space group *Cmce*) that can be modelled as a sequence of AlB_2-type slabs, quadrangular antiprismatic slabs, and distorted αPo-type slabs propagating along the crystallographic *c* direction. The low-temperature physical properties of Yb_2PdGe_6 were determined by means of magnetic susceptibility and electrical resistivity measurements. The compound was characterized as an intermediate valent material because of a highly unstable 4*f* shell of Yb ions.

1. Introduction

Since several years, Yb-bearing intermetallics have attracted much attention owing to their nontrivial physical properties at low temperatures, governed by hybridization between 4*f*-orbitals of Yb atoms and conduction band states. Strong electronic correlations in these materials bring about various electronic ground states and finite-temperature characteristics typical for Kondo lattices, heavy fermions, non-Fermi-liquids, spin and valence fluctuation systems. Most remarkably, the emergence of heavy-fermion superconductivity has also been observed, so far solely in $YbAlB_4$ [1].

For the first time the crystal structure of the title Yb_2PdGe_6 compound was determined in studies of the ternary Yb-Pd-Ge system [2]. Later it was confirmed in the work of Sologub et al. [3] in the frame of the R_2TGe_6 series (R = Rare Earth, T = Pd,Pt,Cu,Ag,Au). In both papers Yb_2PdGe_6 was reported to crystallize with an orthorhombic Ce_2CuGe_6-type of structure (space group *Amm*2, No. 38), the atomic order of which was derived from X-ray (CuKα) powder data collected at $24 \leq 2\Theta \leq 115^\circ$ by Konyk et al. [4]. In the paper by Sologub et al. [3] all other members of the R_2TGe_6 series were also included in the Ce_2CuGe_6-type family. Unit cell dimensions of Yb_2PdGe_6 $a = 4.0755$, $b = 3.9934$, $c = 21.851$ Å as well as its cell volume 355.6 $Å^3$ exhibited positive deviations from the common trend in the R_2TGe_6 series, allowing to suggest a possible valence fluctuation for Yb atoms [3].

Later a more precise single-crystal X-ray diffraction (XRD) method was applied by two different scientific teams, and as a result two other versions for the Yb_2PdGe_6 crystal structure were obtained. Fornasini et al. [5] assigned to this phase an orthorhombic unit cell of the Ce_2GaGe_6-type (space group *Cmce*, No. 64, lattice parameters: $a = 8.142$ Å, $b = 7.980$ Å, $c = 21.829$ Å, $V = 1418.3$ $Å^3$, $Z = 8$). In turn, a single-crystal XRD study by Rizzoli et al. [6] yielded for Yb_2PdGe_6 an orthorhombic crystal structure as a defective version of $SmNiGe_3$-type (space group *Cmmm*, No. 63, $a = 3.996$ Å, $b = 21.880$ Å, $c = 4.076$ Å, $V = 356.4$ $Å^3$, $Z = 4$).

The main aim of our work was to verify the proposed structural models on bulk single phase material by means of powder XRD technique. As the arrangements of atoms in all three variants are very close to each other, only few weak Bragg peaks can be used to discriminate between the models. Nevertheless, we have recently demonstrated for a similar compound Dy_2PdGe_6 [7] that such a verification is fully feasible. It is well known that preparation of the Yb-containing intermetallics in a single phase state is not a simple task due to intensive vaporization of metallic Yb, having a low boiling point at 1193 °C [8]. As the pure Yb_2PdGe_6 compound was successfully obtained, we for the first time, determined the low-temperature magnetic behavior in Yb_2PdGe_6 and the results of our study are presented in this paper.

* Corresponding author.
E-mail address: avgri@mail.ru (A.V. Gribanov).

http://dx.doi.org/10.1016/j.jallcom.2016.06.229
0925-8388/

2. Experimental details

A polycrystalline sample of nominal composition $Yb_{22.2}Pd_{11.1}Ge_{66.7}$ (at. %) was prepared from pure elements (Yb 99.85, Pd 99.99, and Ge 99.999 mass %) by means of arc-melting under argon. The ingot was turned over and remelted as many as 25 times, with adding some excess of Yb at each step. Subsequently, the button was annealed in an evacuated quartz tube at 730 °C for 30 days, followed by quenching in cold water.

Chemical composition and microstructure of the annealed material were examined on a Carl Zeiss LEO EVO 50XVP scanning electron microscope (SEM) equipped with a Link EDX INCA Energy 450 system (Q-BSD detector). The standard deviations for the composition derived did not exceed 0.9 atom % for each element.

The crystal structure of Yb_2PdGe_6 was studied by powder XRD at room temperature using a STOE STADI P transmission diffractometer with monochromatized $CuK_{\alpha1}$ radiation ($\lambda = 1.54056$ Å) and a linear position-sensitive detector. The lattice parameters were calculated using the program STOE-WinXpow [9]. Quantitative Rietveld refinement of the XRD pattern was performed with the FULLPROF program [10,11], employing internal tables for X-ray atomic form factors. Crystal structure and atom polyhedra were visualized using the program DIAMOND [12].

The magnetic study was carried out in the temperature range 1.72–400 K and in external fields up to 5 T using a Quantum Design SQUID magnetometer. The electrical resistivity was measured over the temperature interval 4.5–300 K employing a Quantum Design PPMS platform and standard ac four-probe technique.

3. Results and discussion

3.1. Crystal structure

The microprobe analysis revealed a matrix of composition $Yb_{21.8}Pd_{11.5}Ge_{66.7}$ (at. %) and a minor amount of Yb_2O_3. Probably, a tiny partial oxidation of the sample surface occurred during polishing the specimen for the SEM study, which was done in air.

Fig. 1 presents the measured powder XRD pattern of Yb_2PdGe_6 and its Rietveld analysis using the Ce_2GaGe_6-type model. The refined lattice parameters ($a = 8.1192$ (6), $b = 7.9579$ (5), $c = 21.736$ (2) Å, $V = 1404.4$ (2) Å^3), are in good agreement with the data reported by Fornasini et al. [5]. The correctness of the assumed structural model is further confirmed by the presence in the XRD pattern of the Bragg peaks at $2\theta = 17.54$, 19.80, 29.18, 35.26, 35.78, 35.98 and 37.20 deg (see the inset to Fig. 1), which are expected for the Ce_2GaGe_6-type unit cell, however, not allowed for the Ce_2CuGe_6- and $SmNiGe_3$-types structure proposed earlier for Yb_2PdGe_6 [3,6]. Details on the Rietveld refinement and the crystallographic data obtained are gathered in Table 1. In turn, the refined atomic coordinates and equivalent isotropic displacement parameters are given in Table 2, while the selected interatomic distances are listed in Table 3.

In our work the Ce_2GaGe_6-type was observed in both as-cast and annealed (730 °C) specimens. Similarly, Fornasini et al. [5] selected a suitable single crystal from the annealed (740 °C) alloy. So, one can assume that this structure type is the high-temperature modification. In turn, the $SmNiGe_3$-type structure was detected [6] after annealing at lower temperature (600 °C), and thus may be assumed to be the low-temperature modification. The Ce_2CuGe_6 model was also observed after annealing at 600 °C [2,3] but it seems to be less reliable due to absence of its confirmation from singe-crystal XRD.

In our work, Rietveld refinement of the XRD powder pattern revealed some disorder for the Pd-site. According to the refinement two cases are possible: partial occupation with Pd-atoms (site occupation factor is 0.92) or full occupation with a mixture of (0.74 Pd + 0.26 Ge) atoms. In the former case the chemical composition from refinement agrees well with EDX measurements. while some inaccuracy of the B_{iso} value for that crystallographic position may be explained as arising from imperfections of the crystal structure. This version seems more preferable, so we chose it as correct (Table 3). In the latter case the chemical composition should be significantly shifted from the 2:1:6 ratio enhancing the Ge-content – up to $Yb_{22.2}Pd_{8.3}Ge_{69.5}$ (at.%), which is in contrast to our EDX measurements (see Table 3). That is why we didn't accept this variant.

The crystallographic unit cell of Yb_2PdGe_6 is schematically shown in Fig. 2. It can be viewed as a sequence of quadrangular antiprismatic slabs (I), distorted α-Po type slabs (II), and AlB_2 type slabs (III), arranged along the *c*-direction. Each atom has its own

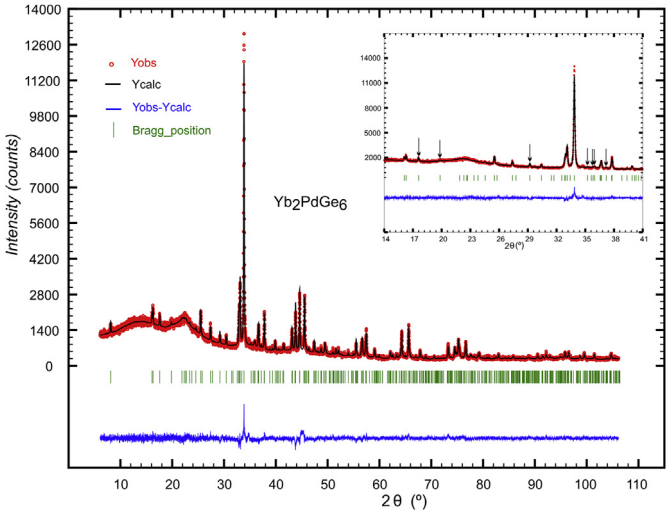

Fig. 1. Rietveld refinement (solid line) of the X-ray powder diffraction pattern of Yb_2PdGe_6. Ticks mark the positions of the Bragg peaks. The bottom line is the difference pattern. Inset: enlarged part of the low-angle XRD pattern of Yb_2PdGe_6. Arrows mark the weak reflexes of the Ce_2GaGe_6 model, which are not allowed for the $SmNiGe_3$- and Ce_2CuGe_6-types structure.

Table 1
X-ray crystallographic data and structure refinement parameters for Yb_2PdGe_6.

Alloy composition [at.%]	$Yb_{22.2}Pd_{11.1}Ge_{66.7}$
Composition from EDX analysis	$Yb_{21.8}Pd_{11.5}Ge_{66.7}$
Composition from powder XRD data	$Yb_{22.4}Pd_{10.3}Ge_{67.3}$
Prototype	Ce_2GaGe_6
Space group	*Cmce*
Pearson symbol	*oC*72
Lattice parameters [Å]	
a	8.1192 (6)
b	7.9579 (5)
c	21.736 (2)
Cell volume [Å^3]	1404.4 (3)
Chemical formula	$Yb_2Pd_{(1-x)}Ge_6$ [x = 0.08 (1)]
Formula weight, [g/mol]	888.02
Number of formula units in unit cell, Z	8
Calculated density [g/cm^3]	8.40
2θ range [°]	$6 \le 2\Theta \le 106$
Reflections in refinement	486
Number of variables	31
$R_F = \Sigma\|F_{oi}-F_{ci}\|/\Sigma F_{oi}$	0.105
$R_B = \Sigma\|I_{o,h}-I_{c,h}\|/\Sigma\|I_{o,h}\|$	0.137
$R_P = \Sigma\|y_{oi}-y_{ci}\|/\Sigma\|y_{oi}\|$	0.060
$R_{wP} = [\Sigma w_i\|y_{oi}-y_{ci}\|^2/\Sigma w_i\|y_{oi}\|^2]^{1/2}$	0.078
$\chi^2 = (R_{wP}/R_e)^2$	4.26

Table 2
Atomic coordinates and equivalent isotropic displacement parameters for Yb_2PdGe_6.

Atom	Wyckoff position	x/a	y/b	z/c	B_{iso} (Å^2)	Occ.
Yb	16g	0.2511 (5)	0.373 (3)	0.08254 (8)	1.37 (6)	1
Pd	8f	0	0.1298 (14)	0.1383 (2)	0.4 (2)	0.92 (1)
Ge1	16g	0.2675 (9)	0.126 (4)	0.1954 (2)	0.63 (7)	1
Ge2	8f	0	0.127 (3)	0.4547 (3)	0.63 (7)	1
Ge3	8f	0	0.128 (3)	0.0271 (3)	0.63 (7)	1
Ge4	8f	0	0.355 (3)	0.3043 (4)	0.63 (7)	1
Ge5	8f	0	0.393 (3)	0.1935 (4)	0.63 (7)	1

Table 3
Selected interatomic distances and coordination numbers (CN) of atoms in the unit cell of Yb_2PdGe_6.

		d (Å)	CN			d (Å)	CN
Yb	– Ge2	2.9304		Ge2	– Ge3	2.5084	
	– Ge2	2.9801			– Ge2	2.8170	
	– Pd	3.0624			– 2 Yb	2.9304	8
	– Ge3	3.0692			– 2 Yb	2.9801	
	– Ge3	3.1062			– 2 Yb	3.4466	
	– Pd	3.1187		Ge3	– Ge3	2.3505	
	– Ge3	3.1236	12		– Pd	2.4190	
	– Ge1	3.1460			– Ge2	2.5084	9
	– Ge5	3.1626			– 2 Yb	3.0692	
	– Ge1	3.1778			–2 Yb	3.1062	
	– Ge4	3.1862			– 2 Yb	3.1236	
	– Ge2	3.4466					
Pd	– Ge5	2.4119		Ge4	– Ge5	2.4271	
	– Ge3	2.4190			– Pd	2.5191	8
	– 2 Ge1	2.5010	9		– 2 Ge1	2.6213	
	– Ge4	2.5191			– 2 Ge1	3.0633	
	– 2 Yb	3.0624			– 2 Yb	3.1862	
	– 2 Yb	3.1187					
Ge1	– Ge1	2.3900		Ge5	– Pd	2.4119	
	– Pd	2.5010			– Ge4	2.4271	
	– Ge4	2.6213			– 2 Ge1	2.6494	8
	– Ge5	2.6494	8		– 2 Ge1	3.0356	
	– Ge5	3.0356			– 2 Yb	3.1626	
	– Ge4	3.0633					
	– Yb	3.1460					
	– Yb	3.1778					

crystallographic position (one position for Yb atoms). Similar to the $SmNiGe_3$-type modification, our powder XRD experiment yielded a slightly disordered Pd-site. All the other atomic sites are fully occupied. The observed interatomic distances are similar to those in related intermetallics. A detailed description of the atomic polyhedra in the Ce_2GaGe_6-type structure can be found in Ref. [7].

All three types of structure – Ce_2CuGe_6, Ce_2GaGe_6, and $SmNiGe_3$, – are very close to each other. The critical review of their atomic orders, as well as that of the related monoclinic La_2AlGe_6 compound was reported by Zhao et al. [13] (in detail) and in Ref. [6] (in brief).

3.2. Physical properties

Fig. 3 displays the measured magnetic data of Yb_2PdGe_6. The compound exhibits a weakly temperature dependent (except for temperatures below ca. 50 K) magnetic susceptibility of about 1.5×10^{-3} emu/mole, and a paramagnetic-like field variation of the low-temperature magnetization that remains small in the strongest magnetic fields applied (see the inset to Fig. 3). These features, and especially a broad hump in $\chi_m(T)$ at elevated temperatures, hint at an unstable 4*f* electronic shell in the Yb ions, characteristic of intermediate valence (IV) materials. The magnetic behavior in IV compounds can be analyzed in terms of the interconfiguration fluctuation model (ICF) [14] that predicts for Yb-bearing systems the magnetic susceptibility

$$\chi_{IV}(T) = \frac{N\mu_{eff}^2[1-\nu(T)]}{3k_B\left(T+T_{sf}\right)} \tag{1}$$

with $\nu(T)$ being a temperature-dependent mean occupation of the electronic ground state

$$\nu(T) = \frac{1}{1+8\exp\left[-E_{ex}/k_B\left(T+T_{sf}\right)\right]}, \tag{2}$$

where $\mu_{eff} = 4.54\ \mu_B$ is the effective magnetic moment of the Yb^{3+} ion, T_{sf} stands for the temperature of spin fluctuations, while E_{ex} denotes the energy separation between the nonmagnetic $4f^{14}$ ground state from the magnetic $4f^{13}$ excited state.

At low temperatures, $\chi_{IV}(T)$ tends to a plateau, and in the limit $T \to 0$, it saturates at a value that depends on both T_{sf} and E_{ex}. However, as can be inferred from Fig. 3, the magnetic susceptibility of Yb_2PdGe_6 rapidly increases below about 50 K. This feature, commonly observed for IV systems, likely arises because of some small amount of paramagnetic impurity present in the specimen studied, here probably Yb_2O_3, which bears trivalent Yb ions. This spurious contribution can be represented by a Curie-Weiss law

$$\chi_{imp}(T) = \frac{C_{imp}}{T-\theta_{imp}}, \tag{3}$$

with $C_{imp} = nC_{Yb3+}$ ($C_{Yb3+} = \mu_{eff}^2/8$) where n is the impurity concentration in the sample measured. The experimental $\chi_m(T)$ data were analyzed in terms of the sum $\chi_m(T) = \chi_{IV}(T) + \chi_{imp}(T)$. The result of least-squares fitting of the above equations to the experimental data of Yb_2PdGe_6 is shown in Fig. 3 by the solid line. In the entire temperature range measured, a very good approximation of $\chi_m(T)$ was achieved. The parameters obtained are: $T_{sf} = 350$ (9) K, $E_{ex} = 1660$ (30) K, $C_{imp} = 0.036$ (9) emu K/mole, and $\theta_{imp} = -9.8$ (7) K. Assuming that the impurity contribution comes exclusively from uncompensated Yb^{3+} ions one can estimate the impurity content in the sample measured to be about 1 at% Yb^{3+} ions per mole. The estimated magnitude of E_{ex} is rather large, hence

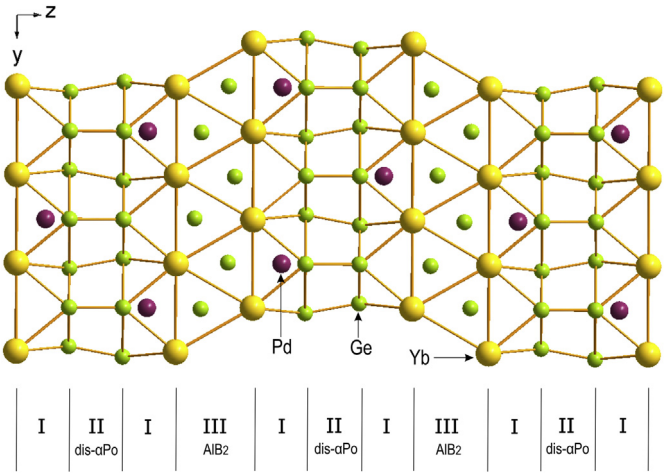

Fig. 2. Packing of atomic layers in the crystal structure of Yb_2PdGe_6.

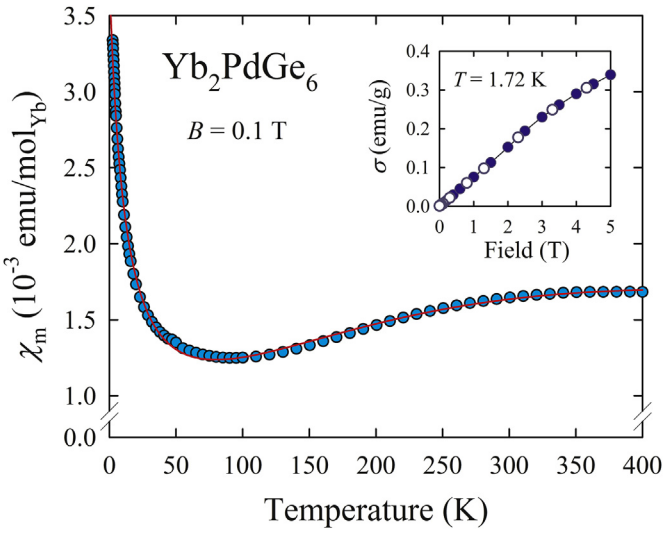

Fig. 3. Temperature dependence of the molar magnetic susceptibility of Yb_2PdGe_6 measured in a magnetic field of 0.1 T. The solid line is the least-squares fit discussed in the text. Inset: magnetic field variation of the magnetization in Yb_2PdGe_6 taken at 1.72 K with increasing (full circles) and decreasing (open circles) field.

indicates that the magnetic $4f^{13}$ configuration is quite distant in energy from the nonmagnetic $4f^{14}$ ground state. Accordingly, the ICF model yields for Yb_2PdGe_6 an effective Yb valence of only +2.07 at 2 K. With increasing temperature, the excited state becomes thermally populated and the valence increases reaching at 300 K a value of +2.38.

The temperature variation of the electrical resistivity of Yb_2PdGe_6 is shown in Fig. 4. The compound exhibits metallic conductivity with the resistivity of about 140 μΩcm at room temperature and about 17 μΩcm at liquid helium temperature. As displayed in Fig. 4, in the entire temperature range, the experimental $\rho(T)$ curve can be approximated by the Bloch-Grüneisen-Mott (BGM) formula [15].

$$\rho(T) = \rho_0 + 4R\theta_R\left(\frac{T}{\theta_R}\right)^5 \int_0^{\frac{\theta_R}{T}} \frac{x^5 dx}{(e^x - 1)(1 - e^{-x})} + KT^3 \qquad (4)$$

where the first term is the residual resistivity due to scattering conduction electrons on static defects in the crystal lattice, the

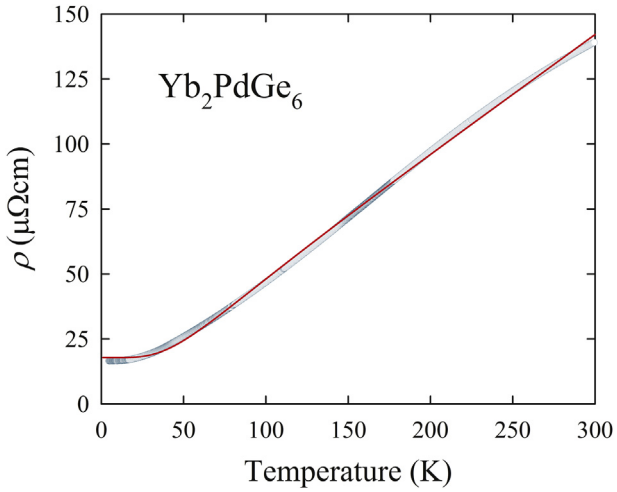

Fig. 4. Temperature dependence of the electrical resistivity of Yb_2PdGe_6. The solid line is the BGM fit discussed in the text.

second term represents electron-phonon scattering processes (θ_R is sometimes considered as a rough measure of the Debye temperature), whereas the third term accounts for Mott-type interband scattering. The BGM parameters obtained for Yb_2PdGe_6 are: $\rho_0 = 17.2\,(4)$ μΩcm, $\theta_R = 254\,(2)$ K, $R = 0.423\,(9)$ μΩcm/K and $K = 8.4\,(3) \times 10^{-8}$ μΩcm/K^3. A featureless $\rho(T)$ dependence with some positive curvature due to electron-electron scattering is usually observed for metallic IV systems [16], and thus the electrical transport in Yb_2PdGe_6 is in concert with the above-described magnetic characteristics of this compound.

4. Conclusions

The ternary germanide Yb_2PdGe_6 forms with the orthorhombic Ce_2GaGe_6-type crystal structure, indicated before by Fornasini et al. [5]. In the crystallographic unit cell, the Yb ions occupy a single position. Their 4*f*-shell is highly unstable, which results in a behavior characteristic of intermediate valence systems. The characteristic energy scale for spin fluctuations amounts to about 350 K and the energy separation between the nonmagnetic ground state $4f^{14}$ and the magnetic $4f^{13}$ configuration is about 1660 K. The average effective Yb-ion valence in Yb_2PdGe_6 increases with increasing temperature and attains about +2.4 near room temperature. The compound exhibits metallic conductivity that varies with temperature in a manner typical for strongly intermediate valent materials.

Acknowledgments

This study was supported by the Russian Foundation for Basic Researches (Grant No 15-03-06767a). X-ray and EDX measurements were performed at User Facilities Center of Lomonosov Moscow State University under support of Ministry of Education and Science of Russia, Contract N16.552.11.7081.

References

[1] S. Nakatsuji, K. Kuga, Y. Machida, T. Tayama, T. Sakakibara, Y. Karaki, H. Ishimoto, S. Yonezawa, Y. Maeno, E. Pearson, G.G. Lonzarich, L. Balicas, H. Lee, Z. Fisk, Nat. Phys. 4 (2008) 603.
[2] Yu.D. Seropegin, O.L. Borisenko, O.I. Bodak, V.N. Nikiforov, M.V. Kovachikova, Yu.V. Kochetkov, J. Alloy. Comp. 216 (1994) 259.
[3] O.L. Sologub, K. Hiebl, P. Rogl, O.I. Bodak, J. Alloy. Comp. 227 (1995) 37.
[4] M.B. Konyk, P.S. Salamakha, O.I. Bodak, V.K. Pecharsky, Kristallografiya 33 (1988) 838.

[5] M.L. Fornasini, P. Manfrinetti, A. Palenzona, Z. Krist. 217 (2002) 173.
[6] C. Rizzoli, O. Sologub, P. Salamakha, J. Alloy. Comp. 351 (2003) L10.
[7] A. Gribanov, S. Safronov, E. Murashova, Y. Seropegin, J. Alloy. Comp. 542 (2012) 28.
[8] J. Emsley, The Elements, Oxford University Press, Oxford (UK), 1999.
[9] STOE WINXPOW (Version 1.06), Stoe & Cie GmbH, Darmstadt, Germany, 1999.
[10] J. Rodriguez-Carvajal, Abstracts of the Satellite Meeting on Powder Diffraction of the XV Congress of the IUCr, 1990, p. 127. Toulouse, France.
[11] T. Roisnel, J. Rodriguez-Carvajal, Materials science forum, in: Proceedings of the European Powder Diffraction Conference, 2008, p. 118.
[12] K. Brandenburg, DIAMOND. Release 3.0e, Crystal Impact Gmbh, Bonn, Germany, 2005.
[13] J.T. Zhao, K. Cenzual, E. Parthé, Acta Cryst. C 47 (1991) 1777.
[14] B.C. Sales, D.K. Wohlleben, Phys. Rev. Lett. 35 (1975) 1240.
[15] N.F. Mott, H. Jones, The Theory of the Properties of Metals and Alloys, Oxford University Press, London, 1958.
[16] J.M. Lawrence, P.S. Riseborough, R.D. Parks, Rep. Prog. Phys. 44 (1981) 1.